DETERMINATION OF THE GRAIN GROWTH KINETICS AS A BASE PARAMETER FOR NUMERICAL SIMULATION DEMAND

JAROMIR MORAVEC
Technical University of Liberec, Department of Engineering Technology, Liberec, Czech Republic

DOI: 10.17973/MMSJ.2015_10_201523

e-mail: jaromir.moravec@tul.cz

The grain size is an important parameter influencing not only the material brittleness and strength properties, but also the transformation processes of creep, strength, and fatigue. This present paper is therefore focused on the process description for the experimental determination of the kinetics of grain growth curves temperature dependence. These curves are then used for numerical simulations of grain coarsening in different technological applications such as welding, heat treatment, or slow cooling of large parts. Further it will be demonstrated how obtained curves can be used for the prediction of the grain size in the heat affected zone (HAZ) of multilayer heterogeneous welds of X10CrWMoVNb9-2 and 18Cr9Ni3CuNbN materials and subsequently verified by real welding experiments. The paper will also show the main benefits of using GLEEBLE simulator for verification of the grain coarsening in HAZ of realized welds.

KEYWORDS
grain size, numerical simulation, X10CrWMoVNb9-2 steel, 18Cr9Ni3CuNbN steel, welding, Gleeble

1. INTRODUCTION

In last few years it is possible to see the effort to increase the mathematical description accuracy of the materials behaviour during their technological processing or during their subsequent operational loading. This concerns mainly heat and creep resistant materials used in the energy industry. During the welding and heat treatment of these materials it is possible to observe significant changes in their mechanical, as well as structural properties. In order to assess these changes during the whole process, the thermal simulations of welding and heat treatment are successfully used.

These computations can largely eliminate risks which are connected with unacceptable defect occurrence or it could lead to elimination of inner stresses caused by the process.

In addition to the commonly predicted variables such as temperature and deformation zone fields there are increasing demands for the austenitic grain size prediction. The grain size is a very important material parameter influencing the mechanical and fatigue properties, transformation processes, or physical properties of the particular material. During the numerical prediction of austenitic grain size, the so-called grain growth kinetics curves represent the basic parameter. These curves can be used for both very fast dynamic processes corresponding to temperature cycles in HAZ during welding and for slow processes occurring under constant temperature representing annealing or during slow cooling of large castings or forgings.

The following part of this paper shows the experimental method for obtaining the grain growth kinetics curves for the martensitic steel X10CrWMoVNb9-2 and the austenitic steel 18Cr9Ni3CuNbN and the numerical prediction of austenitic grain size in HAZ for the three-layer heterogeneous weld made of these materials. Subsequently the advantages and disadvantages of verifying numerically predicted results using welding experiment and thermal-mechanical simulator GLEEBLE will be shown.

2. SIMULATION OF AUSTENITIC GRAIN SIZE

For the prediction of austenitic grain growth these days almost exclusively use the method Monte Carlo with Potts generalised model. It is the method based on theories of probability and mathematical statistics. It belongs to the field of optimized algorithms looking for the minimum of the objective function. Basically, the method tries to determine the mean value of a variable which is the result of a random or pseudorandom process. Stochastic methods, where Monte Carlo belongs, are also used in fields such as thermodynamics, physics, mathematics, computer science, meteorology, biology, medicine, artificial intelligence, environment and so on.

Even though the principle of this method was already formulated in the 1950´s and generalised by R. B. Potts in 1952 [Potts 1952], for the two-dimensional simulation of grain growth kinetics was used not until 1984 by A. P. Anderson et al [Anderson 1984] and for bulk simulations in 1989. Nowadays many works deal with the area of simulation and theory of common grain growth in the three-dimensional bulk, especially for single-phase steels.

Thermodynamic driving force for grain growth represents the decreasing of Gibs free surface energy of grain boundaries. By increasing temperature the smaller grains are gradually absorbed by growing grains; therefore total number of grains are decreasing. The lower gradual surface of absorbed gains, the lower total surface energy which contributes to further grains growth [Yue 2009]. During the grain growth the following basic rules apply:

- The grain grows because of displacement grain boundaries and not because they grow together.
- The movement of grain size is intermitted and the movement direction could suddenly change.
- The grain could grow into another one at the expense of its volume.
- The grain consumption is at the expense of others and often increase when grains are almost consumed.
- The curved boundary usually migrates to its curvature centre.
- If the grain boundaries of one phase meet together in angles different than 120 degrees, grains with the acute angle boundary are consumed so that the angle approaches 120 degrees.

The growth of selected grains which absorb smaller grains are connected with increasing the average grain size over time. Therefore the average diameter or the middle grain surface is used as a rate of the grain size for alloys. Basic calculations predicting the grain size are based on the equation for ideal grain growth (1).

$$D^2 - D_0^2 = Kt \tag{1}$$

Where D is the actual grain size, D_0 is the initial grain size, K is the proportional constant that depends on absolute heating temperature, activation energy and t is holding time at the temperature [Khzouz 2011]. This equation is mainly used for simulations where the presumption exists that the system has no defects, does not contain precipitates, and the grain growth is controlled only by diffusion. In cases where mechanisms cause the slowing of kinetics of austenitic grain growth, the grain growth of the ideal equation is generalized by replacing exponent two to variable coefficient m as shown in equation (2). Equation (3) defines the relation between the proportionality constant K and temperature T at which the grain grow [Khzouz 2011].

$$D^2 - D_0^2 = Kt \tag{2}$$

$$K = K_0 e^{-\frac{Q}{RT}} \tag{3}$$

In this equation D is the actual grain size, D_0 is the initial grain size, K is the proportionality constant, T is the heating temperature, Q is the activation energy necessary for the grain growth, K_0 is the total pre-exponential constant which is obtained experimentally together with the activation energy. R is the gas constant, t is holding time at given temperature, and m is variable exponent depending on the grain growth kinetics. It has been experimentally proven that the exponent m varies within the range of 2 to 5 [Giumelli 1995]. In an ideal state, grain growth is controlled only by diffusion. In this case the exponent m = 2 and the equation (1) for ideal grain growth for simulation calculation is used. Furthermore, grain growth can be controlled, for example, by diffusion together with the precipitation phase in growing grains, the exponent m = 3 is used. If the common effect of precipitation and diffusion along grain boundaries is observed, the exponent m = 4 is used [Giumelli 1995]. In the case when the grain growth is mainly influenced by precipitation, the exponent is close to the value m = 5.

The equation (4) is used for the grain size computation in the simulation program SYSWELD. This equation indicates the grain size growth rate. This equation is derived from equations (2) and (3).

$$\dot{D}^m = K_0 \exp\left(-\frac{Q}{RT}\right) \tag{4}$$

The meaning of the symbols in equation (4) is the same as their description in the case of equations (2) and (3). The computational equation is defined for cases where the amount of austenite is constant or it decreases. If there is the case when the amount of austenite grows, into the equation (4) is added the influence of the increasing portion of austenite and transformation rate of this phase. In this case, the calculation of the grain size is realized according to the equation (5).

$$\dot{D}^m = K_0 \exp\left(-\frac{Q}{RT}\right) - \frac{\dot{\lambda}}{\lambda} D^m \qquad \text{for } \dot{\lambda} > 0 \text{ austenite is created} \tag{5}$$

In equation (5) the λ value indicates the austenite proportion while the value $\dot{\lambda}$ shows the transformation rate of this phase. If the austenite is not created, i.e. $\dot{\lambda} \leq 0$, the equation (4) is valid.

3. DETERMINATION OF THE GRAIN GROWTH KINETICS FOR 18CR9NI3CUNBN AND X10CRWMOVNB9-2 STEELS

X10CrWMoVNb9-2 and 18Cr9Ni3CuNbN materials belong among the high-temperature and creep-resistant steels. Steel X10CrWMoVNb9-2, rather known as P92, belongs among martensitic 9–12% Cr steel. This is (9% Cr, 1.75% W, 0.5% Mo) steel alloyed with vanadium and niobium with controlled content of boron and nitrogen. It is the result of Japanese research and its original designation acc. to the Nippon Steel Corporation manufacturer is NF 616. It is the modification of steel P91 by its alloying with 1.7 wt.% W, which leads to the solid solution substitution strengthening and increasing the creep resistance [Svobodova 2009]. Further increase of the creep resistance is achieved by alloying nitrogen and also by vanadium nitride precipitating inside the grain.

Microstructural stability of the steel is positively influenced by the low coarsening rate of $M_{23}C_6$ particles, which is related to the dissolution of boron atoms in the particular phase. During creep loading it can be observed the growth and consequently the coarsening of the particles. The coarsening rate of $M_{23}C_6$ type carbides increases with increasing content of chromium. During the thermal exposure the precipitation of Laves phase occurs. This phase is rich in W and Mo [Svobodova 2009]. Table 1 shows the chemical composition of X10CrWMoVNb9-2 steel determined by the Q4 Tasman spectrometer. X10CrWMoVNb9-2 steels are designed to be used in ultra-supercritical (USC) power plants. Therefore the working temperatures are within the range 600-620 °C and pressures of about 26 MPa. They are widely used steam systems operating in combined cycle. That is due to their high thermal stability and resistance to thermal fatigue during heating and cooling [Hayashi 1998].

	C	Si	Mn	Cr	Mo	Ni	W	V	Cu	Nb	Co
P92	0.101	0.246	0.409	8.939	0.429	–	1.688	0.193	–	0.055	–
S304H	0.090	0.243	0.873	18.810	0.334	8.449	–	0.059	3,515	0.508	0.151

Table 1. Chemical composition of X10CrWMoVNb9-2 and 18Cr9Ni3CuNbN steel [wt. %]

Steel 18Cr9Ni3CuNbN (also known under the name S304H) belongs among the group of high-alloy austenitic steels of type 18% Cr – 9 % Ni. Due to the precipitation hardening, special elements such as Cu, Nb and N are added. It is the austenitic steel with a controlled content of carbon to achieve the resistance even under temperatures 550 °C. Advantage of the austenitic steel 18Cr9Ni3CuNbN is its high corrosion resistance both in oxidizing and reducing environments. It is widely used as the construction material of facilities for the energy industry such as superheaters, heat exchangers, pipes, and other components used in USC power plants. These steels have 3% Cu added which allows their long-term utilization under temperatures of 600 °C [Prabha 2009]. Addition of the nitrogen leads to the material hardening and it is related with the increasing resistance to tensile loading. The creep resistance is increased during precipitation of the Cu-rich phase in the matrix [Sawaragi 1992]. Besides this phase precipitation there is also precipitation of niobium carbo-nitrides resulting in further precipitation hardening. This gradually occurs during the operational loading and after temperature exposure corresponding to approximately 1000 hours before it reaches its maximum. After this hardening process it achieves the hardness up to 246 HV and keeps these values hereafter. This fact was verified during operating conditions under temperature 650 °C for 8000 hours [Tohyama 2001]. The amount of copper varies during the precipitation process while increasing copper content is observed during the aging under temperatures of 650 °C. During this process, other elements such as Fe, Cr, Ni diffuses outside and thus the copper content is further increasing [Cengyu 2011]. Moreover during thermal exposure the diffusion of chromium and expansion of the surface layer of Cr_2O_3 can also be observed. This layer provides very good resistance to oxidation media and decreases its value on minimum. The chemical composition of S304H steel determined by Q4 Tasman spectrometer is shown in Table 1.

To acquire input data for grain size simulation of X10CrWMoVNb9-2 and 18Cr9Ni3CuNbN steels tested specimens were taken from a pipe with the diameter 38 mm and wall thickness 6.3 mm. These specimens were exposed to temperature cycles in the thermal simulator Gleeble 3500 within the temperature range 900–1200°C with temperature increment of 100°C and holding time for 0.5; 2; 4 and 8 hours. The purpose was to acquire input data for determining grain growth kinetics.

Previous works proved that the slower heating rate, the bigger initial size of grain D0 and that is why there was used the heating rate 50°C·s-1 for all the specimens. Due to that, it is possible to vanish the effect of heating on grain coarsening. After holding time expiry the specimens were cooled by copper clamping jaws. Cooling rates down to the temperature 350°C don't fall below 20°C·s^{-1}. Heat treated specimens were cut in the area of control thermocouple, metallographically processed and etched for the visibility of grain boundaries. Specimens of S304H steel were etched in a solution of 80 ml HCl; 13 ml HF and 7 ml HNO_3. Specimens of P92 steel were etched using Villela Bain. All specimens were then digitally scanned and evaluated according to ISO 643 standard using Jefferies planimetric method. The resulting grain size values for both materials are shown in table 2.

Holding temp.	Holding time under given temperature							
	1800 [s]		7200 [s]		14400 [s]		28800 [s]	
	S304H	P92	S304H	P92	S304H	P92	S304H	P92
900 [°C]	0.02063	0.00896	0.02079	0.00942	0.02126	0.01194	0.02143	0.01351
1000 [°C]	0.02081	0.01038	0.02178	0.01197	0.02211	0.01457	0.02396	0.01741
1100 [°C]	0.02835	0.04879	0.03093	0.05379	0.03275	0.05787	0.04113	0.07727
1200 [°C]	0.03078	0.21092	0.03971	0.21655	0.04376	0.22269	0.05114	0.22571

Table 2. Grain size D [mm] for X10CrWMoVNb9-2 and 18Cr9Ni3CuNbN (different temperatures and holding times)

To calculate the grain size it is necessary to determine the total pre-exponential constant K_0 value and activation energy Q for grain growth. During the first phase the initial grain size value D_0 and partial pre-exponential constant K_T are determined for every holding temperature (900 ÷ 1200 °C). The way of obtaining D_0 and K_T for 18Cr9Ni3CuNbN steel is shown in Fig 1. Experimentally obtained average grain size unit for D (Table 2) was written into the graph as square in the time dependence. Each of the tested temperatures are expressed by the trend line and its basic equation by the fitting method. From the trend line slope it is possible to use the value of the partial pre-exponential constant K_T and the initial grain size D_0 for the particular temperature, which is obtained from the fitting line equation at the starting time. The same procedure was applied for obtaining D_0 and K_T values for X10CrWMoVNb9 steel. All measured and computed values for both materials are shown in Table 3.

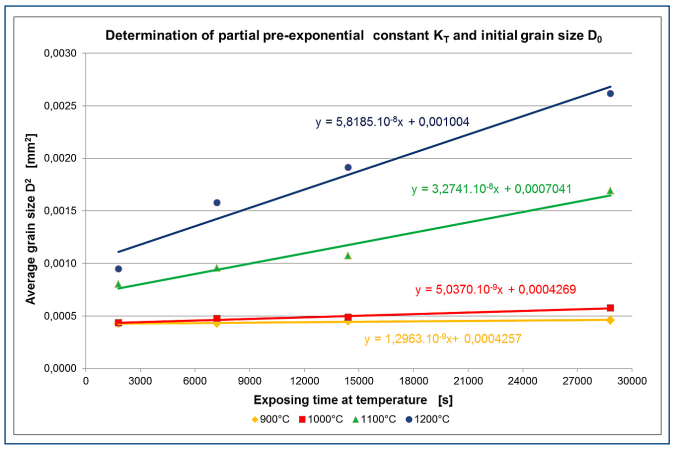

Figure 1. Square dependance of average grain size D_2 on time

18Cr9Ni3CuNbN / X10CrWMoVNb9-2	Holding temperature			
	900 [°C]	1000 [°C]	1100 [°C]	1200 [°C]
18Cr9Ni3CuNbN K_T [mm².s⁻¹]	1.2963.10-9	5.0370.10-9	3.2741.10-8	5.8185.10-8
X10CrWMoVNb9-2 K_T [mm².s⁻¹]	4.0370.10-9	7.3333.10-9	1.3367.10-7	2.3015.10-7
18Cr9Ni3CuNbN D_0 [mm]	0.0004257	0.0004269	0.0007041	0.001004
X10CrWMoVNb9-2 D_0 [mm]	0.0000707	0.0000958	0.0019054	0.0449757
18Cr9Ni3CuNbN Ln K_T [mm².s⁻¹]	-20.4638	-19.1065	-17.2346	-16.6596
X10CrWMoVNb9-2 Ln K_T [mm².s⁻¹]	-19.3278	-18.7308	-15.8279	-15.2845
Both materials T^1 [K]	0.0008525	0.0007855	0.000728	0.0006789

Table 3. Partial pre-exponential values K_T and grain size D_0 for X10CrWMoVNb9-2 and 18Cr9Ni3CuNbN steels

The activation energy Q and the total pre-exponential constants K_0 it is possible to obtain by the way shown in Fig. 2. The logarithm values of the acquired partial pre-exponential constant K_T, which are dependant on reversed values of the absolute holding temperature, are plotted in the graph. Thanks to that the trend line can be created. Its equation can be expressed in the following format (6).

$$y = C \cdot x + B \tag{6}$$

The constant C in equation (6) defines the slope of the trend line, and will be, together with the gas constant R, further used to calculate the activation energy Q according to equation (7). The constant B is used to calculate the total value of the total pre-exponential constants K0 according to equation (8).

$$Q = -(2{,}3 \cdot R \cdot C) \tag{7}$$

$$K_0 = e^B \tag{8}$$

According to the trend line (Fig. 2) and by means of equations (7) and (8), activation energy values Q = 441.1 [kJ.mol⁻¹] of the grain growth for the 18Cr9Ni3CuNbN steel and total pre-exponential constants K_0 = 44,722.10-2 [mm2.s⁻¹] were computed. In the same manner there were determined values Q = 494.7 [kJ.mol⁻¹] and K_0 = 11.057 [mm2.s⁻¹] for the X10CrWMoVNb9-2 steel. This data can be used as input data for simulation programs and according to equation (3) used to define the temperature dependence of proportionality constant K. This curve is also known as curve of the grain growth kinetics. In Fig. 3 are shown curves of grain growth kinetics for both materials. Regarding the optimal display is the y-axis multiplied by 1014. From the Fig. 3 is evident that more intensive grain growth occurs under temperatures after 1200 °C.

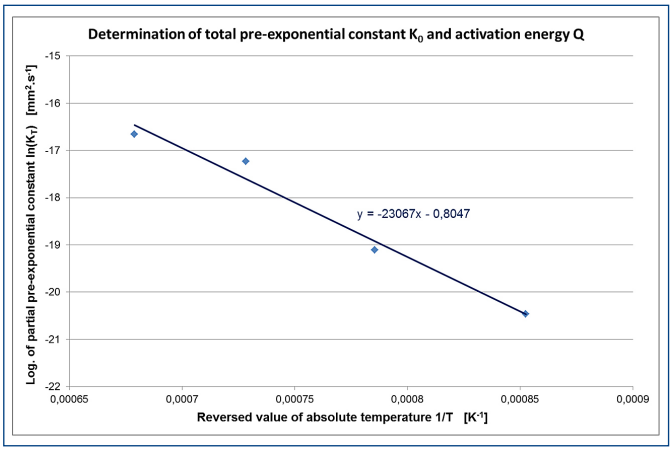

Figure 2. Dependence of proportionality constant K on absolute temperature reversed value

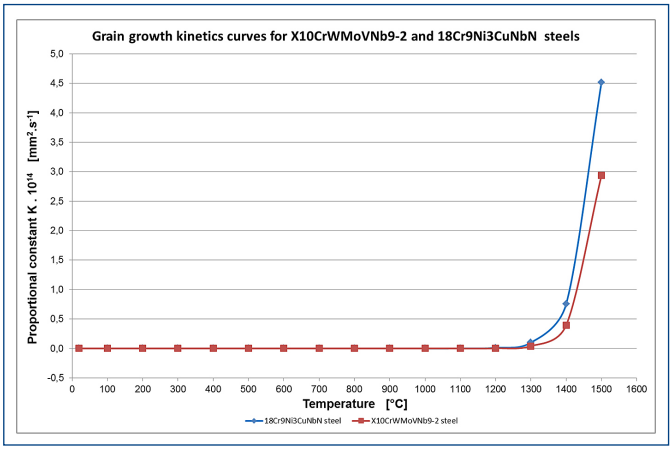

Figure 3. Grain growth kinetic curves K for X10CrWMoVNb9-2 and 18Cr9Ni3CuNbN steel

4. THE SIMULATION OF THE GRAIN COARSENING IN HAZ OF WELDS AND THEIR VERIFICATION

Obtained curves K of grain growth kinetics were used as input data for the grain growth simulation in the SYSWELD program. In order to realize simulation computations and thus to compare the results with the real conditions, welding experiments of X10CrWMoVNb9-2 and 18Cr9Ni3CuNbN steels using method 141 according to the standard ISO 4063 were carried out. Experimental welds were made as three layered weld on the pipe diameter 38, wall thickness 6.3 mm. In order to properly define the experiment boundary conditions, the programmable device with automatic orbital head and wire feeder supplied by the Polysoude company were used for welding. The additional material Thermanit 617 from BÖHLER UDDEHOLM 0.8 mm was also used during welding. The input heat depending on the welding position and the type of weld bead (root, filling, cover) varies within 11 to 19 kJ cm⁻¹. The edges

of the individual weld beads were reciprocally shifted by 120° while the welding directions of the successive beads were reversed. None of the weld beads were finished immediately after 360°C, they all overlapped their edges at least by 10 mm to achieve the melting of material and filling the whole welding profile.

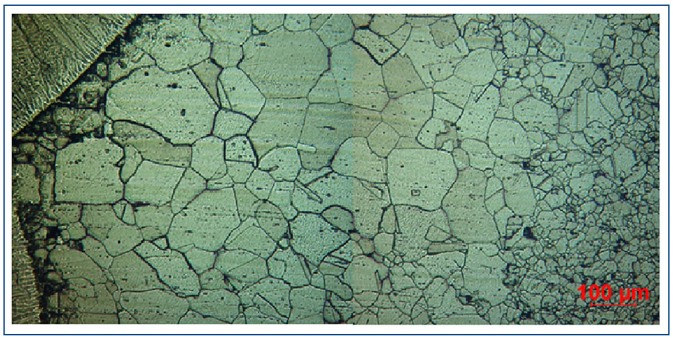

Figure 4. Grain size in HAZ for real weld at the side of 18Cr9Ni3CuNbN steel

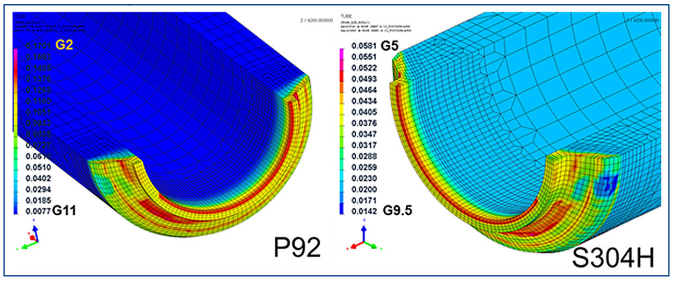

Figure 5. Numerically computed grain sizes for X10CrWMoVNb9-2 and 18Cr9Ni3CuNbN steels

By using the macro scratch pattern of a weld, this defined the geometry of the individual weld beads and created a spatial model with the SYSWELD program. Non-stationary temperature fields of each weld bead were numerically computed using Goldak double-ellipsoidal heat source model by substitution measured, processional and geometrical quantitates into this source. Resulting temperature fields were then used for the calculation of austenitic grain in HAZ. Fig. 4 shows the grain size in HAZ of the real weld on the side of austenitic steel S304H. Fig. 5 shows numerically computed grain sizes in SYSWELD program for the HAZ of both steels.

From Fig. 4 it is evident that there are some problems related with planning and comparison of results. Since it is necessary to compare the grain size in precisely defined distances from the melting boundary, the Jefferies planimetric method cannot be used for the determination of the grain size. As a partial solution the linear intersection method can be used when the equidistant lines are placed in precisely defined distance from the melting boundary. However, this method also has its limitations and inaccuracies.

The ideal way how to verify previously numerically computed results is to use comparative samples made by thermal-mechanical simulator GLEEBLE. By means of this device it is possible to apply the particular welding cycle on the specimen corresponding to the appropriate place in HAZ. Data for thermal cycles can be acquired on the basis of thermocouple data during the experiment or can be generated directly for the particular place in HAZ by usage of simulation program. In this case it is possible to precisely define the inaccuracy of the results of numerical simulations for grain coarsening.

Fig. 6 shows the structure of 18Cr9Ni3CuNbN steel (under 100x magnification) obtained from thermal-mechanical simulator and corresponding the distance from the melting boundary 0.5; 1.5; 2.5 and 3.5 mm. Temperature cycles were taken from simulation calculations. Each verified sample was subjected to three welding cycles which corresponds to the thermal influence by the individual weld beads in particular place of HAZ.

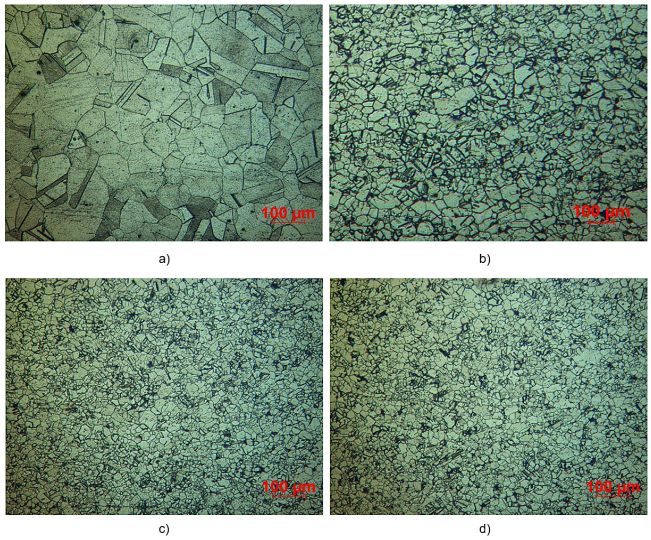

Figure 6. Material structures of 18Cr9Ni3CuNbN steel for specimens loaded by thermal-mechanical simulator corresponding to the distance of the grain boundary a) 0.5 mm; b) 1.5 mm; c) 2.5 mm; d) 3.5 mm.

Table 3 shows the comparison of resulting grain size values in HAZ for real welds and simulation computations in pre-defined points with the distance from the melting boundary 0.5; 1.0; 1.5; 2.0; 2.5; 3.0 and 5.0 mm.

		Distance from the melting boundary						
		0.5	1.0	1.5	2.0	2.5	3.0	5.0
18Cr-9Ni3CuNbN	D_{middle} [mm] – experiment	0.0834	0.0638	0.0272	0.0251	0.0209	0.0193	0,0207
	No. of grains 1/ mm² – exper.	144	246	1352	1587	2289	2685	2334
	No. of grain size G – exper.	G4	G5	G7	G8	G8	G8	G8
	D_{middle} [mm] – simulation	0.0721	0.0579	0.0296	0.0243	0.0204	0.0204	0.0204
	No. of grains 1/ mm² – sim.	192	298	1141	1693	2403	2403	2403
	No. of grain size G – sim.	G4-5	G5	G7	G8	G8	G8	G8
X10CrWMoVNb9-2	D_{middle} [mm] – experiment	0.0964	0.0781	0.0617	0.0439	0.0211	0.0098	0.0076
	No. of grains 1/ mm² – exper.	108	164	263	519	2249	10412	17313
	No. of grain size G – exper.	G4	G4	G5	G6	G8	G10	G11
	D_{middle} [mm] – simulation	0.1046	0.0932	0.0743	0.0472	0.0147	0.0077	0.0077
	No. of grains 1/ mm² – sim.	91	115	181	449	4628	16866	16866
	No. of grain size G – sim.	G3	G4	G4	G6	G9	G11	G11

NOTICE: D_{middle} = middle grain size; No. of grain size G = grain size number evaluated with Jefferies planimetric method; No. of grains 1/ mm² = Number of grain per mm²

Table 3. Comparison of the resulting grain size values in HAZ for real welds and simulation computations

CONCLUSION

As was previously mentioned, the methodical procedure for experimental determination of grain growth curve kinetics can be used both for materials with phase transformation and for single-phase materials. Although the described methodology is based on input experiments with long exposure at a particular temperature, it can be successful with relatively high accuracy in dynamic processes such as grain coarsening numerical simulation in HAZ during welding. The higher accuracy can be achieved during numerical simulations corresponding to long exposures at temperature.

Nevertheless, it is important to take into account several limitations when interpreting results because of their impact on the accuracy of numerically predicted results. The first one concerns the type of material for which the grain size is predicted. For single-phase steels (e.g. austenitic steel 18Cr9Ni3CuNbN) it is possible to simulate any temperature cycle because the grain remains austenitic all the time. For materials with phase transformation it is possible to simulate any temperature cycle

but only in the austenite area. During subsequent cooling over the transformation temperature, the diffusionless martensitic transformation has to be ensured to keep the original size of austenitic grains. During other types of phase transformations the changes of original grains size occur. These changes can influence the final result. This is true especially for verification experiments.

Another variable affecting the final accuracy of simulated results is the value of the exponent m. Therefore, it is important to know if the grain growth is controlled only by diffusion or there is decrease of the grain growth due to the precipitation processes. In case of temperature field simulations is also important to properly define the boundary conditions because the predicted temperature field together, with a defined curve of grain growth kinetics, determines the final size of numerically calculated austenitic grains.

As was already shown in chapter 4 (Fig. 4), macro-scratch patterns of real welds are not suitable for the verification of the grain coarsening in HAZ. That is why it is not possible to use the surface evaluation of the grain size in the particular area according to Jefferies planimetric method. Therefore, it is much more useful and more accurate to use simulated temperature cycles corresponding particular locations in HAZ.

The main advantage of these methodological procedures is the optimization of computational models for the particular material. This allows predicting the results of grain coarsening for other welding procedures with sufficient accuracy. Beside finding the optimal solution it is possible to understand the behaviour and response of material in dependence on its technological processing. Another advantage of mentioned methodical procedure is also the direct determination of the activation energy value. For commonly used commercial software the activation energy value Q is estimated on the base of reciprocal influence of the total pre-exponential constant K_0 and exponent m as it was already mentioned previously by equations (2) and (3).

REFERENCES

[Anderson 1984] Anderson, M. P., Srolovitz, D. J., Grest, G. S., Sahni, P. S. Computer simulation of grain growth – I. Kinetics, Acta Metallurgica, volume 32, issue 5, 1984, pp. 783-791.

[Cengyu 2011] Cengyu, CH., Hongyao, Y., Jianxin, D., Xishan, X., Zhenggiang, C., Xiaofang, Ch., Fusheng, L. Strengthening effect of Cu-rich phase precipitation in 8Cr9Ni3CuNbN austenitic heat-resisting steel. Acta Metallurgica Sinica (Engl. Lett.)Vol.24, April 2011, pp 141–147.

[Giumelli 1995] Giumelli, A. Austenite Grain Growth Kinetics and the Grain Size Distribution. Master of Applied Science Degree, The University of British Columbia. Available from < http://circle.ubc.ca/bitstream/handle/2429/3572/ubc 1995-0157.pdf? Sequ ence=1>

[Hayashi 1998] Hayashi, M. Thermal fatigue behavior of thin walled cylindrical carbon steel specimens in simulated BWR environment. Nuclear Engineering and Design, 1998; 184, pp. 123 – 133.

[Khzouz 2011] Khzouz, E. Grain Growth Kinetics in Steels. Worcester Polytechnic Institute. Degree of Bachelor of Science. Available from < http://www.wpi.edu/Pubs/E-project/Available/E-project-042211104204/unrestricted/MQP_Grain_Growth_Kinetics in _ Steels.pdf>

[Potts 1952] Potts, R. B. Some generalized order-disorder transformations, Proceedings of the Cambridge, Philosophical Society, volume 48, issue 01, 1952, pp. 106-109.

[Prabha 2009] Prabha, B., Sundaramoorthy, P., Suresh, S., Manimozhi, S., Ravishankar, B. Studies on Stress Corrosion Cracking of Super 304H Austenitic Stainless Steel. Journal of Materials Engineering and Performance. December 2009, Volume 18, Issue 9, pp 1294–1299.

[Sawaragi 1992] Sawaragi, Y., Ogawa, K., Kato, S., Natori, A., Hirano, S. Development of the economical 18-8 stainless steel (SUPER 304H) having high elevated temperature strength for fossil fired boilers. The Sumitomo search, No. 48, 1992, pp. 50-58.

[Svobodova 2009] Svobodova, M., Douda, J., Cmakal, J., Sopousek, J., Dubsky, J. Homogennous and heterogennous weld joints of creep resistante steels. In METAL 2009.

[Tohyama 2001] Tohyama, A., Hayakawa, H., Minami, Y. Development of high strength steel boiler tube (TEMPALOY AA-1). NKK Technical review, No.84, 2001, p. 30-35.

[Yue 2009] Yue, Ch., Zhang, L., Liao, S., Gao, H. Kinetic analysis of the austenite grain growth in GCr15 steel, Journal of Materials Engineering and Performance, vol. 19, no. 1, 2009, pp. 112-115.

CONTACT:

Ing. Jaromir Moravec, Ph.D., EWE.
Technical university of Liberec
Department of Engineering technology
Studentska 1402/2, 461 17 Liberec 1, Czech Republic
tel.: +420 485 353 341
e-mail: jaromir.moravec@tul.cz
www.tul.cz